Unified Power Quality Conditioner: The Indirect Matrix Converter Solution

M. P. Alves[(1)], T. Geury[(1,2,3)], S.F. Pinto[(1,3)]
[(1)]INESC-ID, [(2)]FRIA scholarship, BEAMS Energy, École polytechnique de Bruxelles,
[(3)]DEEC, Instituto Superior Técnico, Universidade de Lisboa,
Av. Rovisco Pais, 1, 1049-001 Lisboa
PORTUGAL
miguel.pires.alves@tecnico.ulisboa.pt thomas.geury@ulb.ac.be soniafp@tecnico.ulisboa.pt

Abstract: - Power Quality (PQ) parameters such as voltage RMS value, Total Harmonic Distortion (THD), and Power Factor (PF) are main topics to be considered in the connection of sensitive loads to the grid. In this paper, a Unified Power Quality Conditioner (UPQC) based on an Indirect Matrix Converter (IMC) is proposed to address some PQ issues as mitigation of voltage harmonics and compensation of sags and swells when supplying a sensitive load. Also, it allows the mitigation of grid current harmonics in the Point of Common Coupling (PCC). The control of the converter is performed using the sliding mode control method, associated to the state-space vector representation, allowing fast response times to disturbances in the grid. The whole system is tested in MATLAB Simulink software, and the obtained results show that it guarantees PQ improvement in the PCC.

Key-Words: - Power Quality, Unified Power Quality Conditioner, Indirect Matrix Converter, Sliding Mode Control.

1 Introduction

Power Quality (PQ) has become a relevant topic in the last decades, and PQ parameters as the voltage RMS value and Total Harmonic Distortion (THD) are bounded by international standards, e.g. EN 50160 [1].

Nowadays, electrical systems are more complex than a few decades ago, and every single disturbance or failure may lead to severe consequences, especially in sensitive loads. In fact, some PQ issues may be responsible for the destruction of sensitive equipment or the interruption of some industrial processes, usually resulting in high losses.

A few decades ago, PQ was often associated to continuity of service, that is, interruptions and their duration. However, in recent decades, the quality of the voltage waveforms has become more relevant, and parameters such as the voltage RMS value, the voltage and current THD, or the Power Factor (P_F) are now important PQ indicators.

Until the 1970s the majority of the loads, mainly for lightning and heating, were linear. However, in recent decades the percentage of nonlinear loads has increased due to the generalized use of electronic equipment by industry and domestic consumers. These nonlinear loads are the main source of current harmonics, which result in voltage harmonics, mainly due to the reactance of the grid cables.

One of the ways to mitigate PQ issues is to use power electronic converters with a shunt connection to the grid [2], series connection [3] or both shunt an series [4], [5], with or without [6] storage requirements.

In this paper a Unified Power Quality Conditioner (UPQC), allowing both shunt and series connection to the grid, and based on an Indirect Matrix Converter (IMC) with minimum filtering and no storage requirements is proposed.

Non-linear control approaches usually guarantee better dynamic performance [7] and, in this work, a non-linear direct sliding mode control approach will be used [8], [9].

In this context, the main focus of this paper is to address the following PQ parameters: voltage RMS value and voltage Total Harmonic Distortion (THD_v) in the sensitive load, as well as the Power Factor (P_F) and current Total Harmonic Distortion (THD_i) in the connection to the grid.

Standard EN50160 [1] defines the characteristics of voltage, at the point of supply to the consumer in the Low Voltage (LV), Medium Voltage (MV) and High Voltage (HV) grid. It only considers the harmonics up to the 40th order. Consequently, the

voltage RMS value (V) and THD_v can be obtained from (1) and (2) respectively.

$$V = \sqrt{\sum_{n=1}^{40} V_n^2} \tag{1}$$

$$THD_v(\%) = \frac{\sqrt{\sum_{n=2}^{40} V_n^2}}{V_1} \times 100 \tag{2}$$

The Power Factor P_F can be obtained from (3), where φ_1 is the displacement factor between the fundamental harmonic of the voltage and the current. As the THD_i is usually much higher than the THD_v, the contribution of the latter to the P_F can usually be neglected.

$$\begin{aligned} P_F &= \frac{1}{\sqrt{1+THD_v^2}} \frac{1}{\sqrt{1+THD_i^2}} \cos\varphi_1 \approx \\ &\approx \frac{1}{\sqrt{1+THD_i^2}} \cos\varphi_1 \end{aligned} \tag{3}$$

The UPQC series transformer (Fig. 1) acts as a Dynamic Voltage Restorer (DVR) [3] guaranteeing the mitigation of voltage harmonics, as well as the simultaneous compensation of sags and swells in the PCC, where a three phase sensitive load is connected. Additionally, the UPQC shunt connection allows for minimum THD_i, acting as an active power filter and allowing P_F compensation in the connection to the grid.

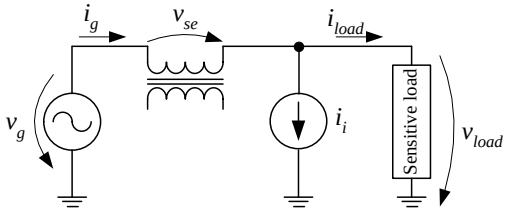

Fig. 1. Single phase equivalent of the proposed UPQC.

2 Proposed System

The proposed UPQC based on an IMC, obtained from the association of a 3x2 Matrix Converter (MC) and a Voltage Source Converter (VSC) is presented in Fig. 2. The proposed system also includes a three-phase series transformer, as well as filtering inductors and capacitors.

The main goal of the UPQC is: a) to guarantee that the RMS value of the voltage V_{load} in the PCC is bounded by the limits defined in standard EN50160; b) to minimize the harmonic content of the grid currents i_g, guaranteeing a nearly unitary power factor.

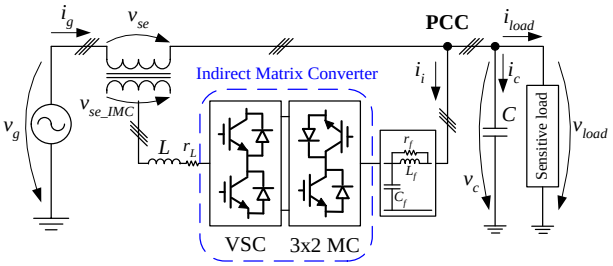

Fig. 2. UPQC system representation.

2.1 Series transformer

The series transformer is used to connect the IMC to the electrical grid. From Fig. 2 it is possible to obtain the voltage to be applied by the series transformer (4):

$$v_{se\_abc}(t) = v_{grid\_abc}(t) - v_{load\_abc}(t) \tag{4}$$

The UPQC should be able to mitigate sags or swells up to 25% of the grid rated voltage value. Then, considering that the transformer turns ratio is unitary, the maximum voltage to be applied by the series transformer is (5), where V_{se} is the RMS value of the voltage applied by the series transformer, and V_{gN} is the nominal RMS value of the grid voltage (V_{gN}=230V):

$$V_{se\_IMC} = V_{se} = 0.25\, V_{gN} \tag{5}$$

From the load voltage V_{load} and the maximum current demanded by the load I_{load_max} it is possible to obtain the UPQC maximum apparent power S_{max} (6). Then, from (5) and (6), the apparent power of the series transformer can be obtained from (7).

$$S_{\max} = 3V_{load}\ I_{load\_\max} \tag{6}$$

$$S_{se} = 3V_{se}\ I_{load\_\max} = 0.25\, S_{\max} \tag{7}$$

2.2 Indirect Matrix Converter

A detailed representation of the IMC [10] to be used in the UPQC (Fig. 2) is represented in Fig. 3.

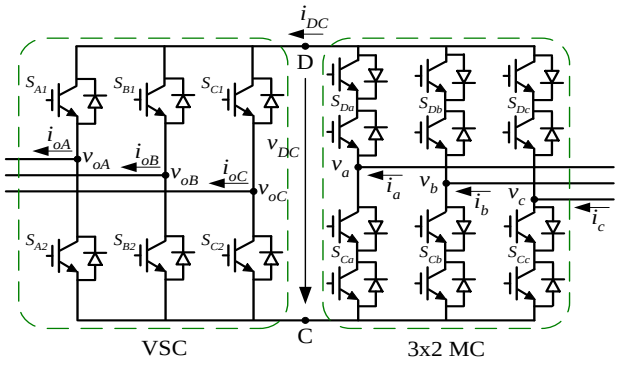

Fig. 3. Topology of the IMC.

From Fig. 3 the matrix which describes the states of the 3x2 MC is (8), where each switch S_{kj} $\left(k \in \{D,C\} \text{ and } j \in \{a,b,c\}\right)$ is represented by a binary variable with two possible states: S_{kj}=1 when the switch is ON, and S_{kj}=0 when the switch is OFF.

$$\mathbf{S_{MC}} = \begin{bmatrix} S_{Da} & S_{Db} & S_{Dc} \\ S_{Ca} & S_{Cb} & S_{Cc} \end{bmatrix} \quad \sum_{j=a}^{c} S_{kj} = 1; \quad k \in \{D,C\} \quad (8)$$

Table I presents all the possible switching combinations for the 3x2 MC, and the resultant space vectors.

TABLE I. SWITCHING COMBINATIONS FOR THE 3X2 MC

	S_{Da}	S_{Db}	S_{Dc}	S_{Ca}	S_{Cb}	S_{Cc}	v_{DC}	i_a	i_b	i_c	$\|I\|$	μ
M1	1	0	0	0	0	1	$-v_{ca}$	i_{DC}	0	$-i_{DC}$	$-\sqrt{2}i_{DC}$	7π/6
M2	0	1	0	0	0	1	v_{bc}	0	i_{DC}	$-i_{DC}$	$\sqrt{2}i_{DC}$	π/2
M3	0	1	0	1	0	0	$-v_{ab}$	$-i_{DC}$	i_{DC}	0	$-\sqrt{2}i_{DC}$	-π/6
M4	0	0	1	1	0	0	v_{ca}	$-i_{DC}$	0	i_{DC}	$\sqrt{2}i_{DC}$	7π/6
M5	0	0	1	0	1	0	$-v_{bc}$	0	$-i_{DC}$	i_{DC}	$-\sqrt{2}i_{DC}$	π/2
M6	1	0	0	0	1	0	v_{ab}	i_{DC}	$-i_{DC}$	0	$\sqrt{2}i_{DC}$	-π/6
M7	1	0	0	1	0	0	0	0	0	0	-	-
M8	0	1	0	0	1	0	0	0	0	0	-	-
M9	0	0	1	0	0	1	0	0	0	0	-	-

The matrix which describes the states of the VSC is (9), where each switch S_{mn} $(m \in \{A,B,C\}$ and $n \in \{1,2\})$ is represented by a binary variable with two possible states: S_{mn}=1 when the switch is ON, and S_{mn}=0 when the switch is OFF.

$$\mathbf{S_{VSC}} = \begin{bmatrix} S_{A1} & S_{A2} \\ S_{B1} & S_{B2} \\ S_{C1} & S_{C2} \end{bmatrix} \quad \sum_{n=1}^{2} S_{mn} = 1 \quad m \in \{A,B,C\} \quad (9)$$

Table II presents all the possible switching combinations for the VSC, and the resultant space vectors.

TABLE II. SWITCHING COMBINATIONS FOR THE VSC

	S_{A1}	S_{A2}	S_{B1}	S_{B2}	S_{C1}	S_{C2}	v_{oAB}	v_{oBC}	v_{oCA}	i_{DC}	$\|\mathbf{V_o}\|$	δ
V1	1	0	0	1	0	1	v_{DC}	0	$-v_{DC}$	i_{oA}	$\sqrt{2}v_{DC}$	π/6
V2	1	0	1	0	0	1	0	v_{DC}	$-v_{DC}$	$-i_{oC}$	$-\sqrt{2}v_{DC}$	3π/2
V3	0	1	1	0	0	1	$-v_{DC}$	v_{DC}	0	i_{oB}	$\sqrt{2}v_{DC}$	5π/6
V4	0	1	1	0	1	0	$-v_{DC}$	0	v_{DC}	$-i_{oA}$	$-\sqrt{2}v_{DC}$	π/6
V5	0	1	0	1	1	0	0	$-v_{DC}$	v_{DC}	i_{oC}	$\sqrt{2}v_{DC}$	3π/2
V6	1	0	0	1	1	0	v_{DC}	$-v_{DC}$	0	$-i_{oB}$	$-\sqrt{2}v_{DC}$	5π/6
V7	0	1	0	1	0	1	0	0	0	0	-	-
V8	1	0	1	0	1	0	0	0	0	0	-	-

From (8) and (9) it is possible to obtain the matrix that relates the IMC input and output voltages and currents (10) [9]:

$$\mathbf{S_{IMC}} = \mathbf{S_{MC}}\,\mathbf{S_{VSC}} \quad (10)$$

From (10), the IMC output voltages (v_{oA}, v_{oB}, v_{oC}) can be related to the input voltages (v_a, v_b, v_c) (11). Also, the input currents (i_a, i_b, i_c) can be related to the output currents (i_{oA}, i_{oB}, i_{oC}) (11).

$$\begin{bmatrix} v_{oA} & v_{oB} & v_{oC} \end{bmatrix}^T = \mathbf{S_{IMC}} \begin{bmatrix} v_a & v_b & v_c \end{bmatrix}^T$$
$$\begin{bmatrix} i_a & i_b & i_c \end{bmatrix}^T = \mathbf{S}_{\mathbf{IMC}}^T \begin{bmatrix} i_{oA} & i_{oB} & i_{oC} \end{bmatrix}^T \quad (11)$$

2.3 IMC input filter

The IMC is connected to the electric grid through a second order filter with a damping resistor (L_f, r_f and C_f) (Fig. 4) [11]. This filter is used to minimize the high frequency harmonics originated by the switching process of the IMC's semiconductors, and the values used for the IMC filter parameters are presented in table III.

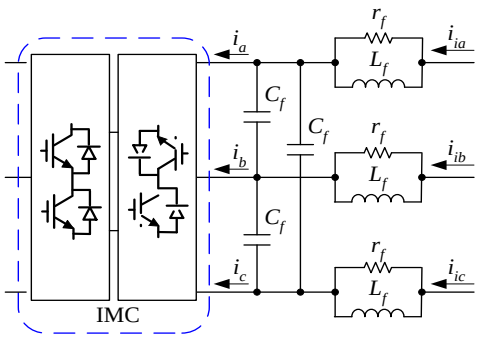

Fig. 4. Three-phase IMC input filter.

TABLE III. INDIRECT MATRIX CONVERTER INPUT FILTER PARAMETERS

Filter parameters		
L_f **[mH]**	r_f **[Ω]**	C_f **[μF]**
3.33	0.26	8.48

3 Controllers Design

In this chapter the voltage controllers and the grid side P_F controllers are designed. The voltage controllers will establish the references for the IMC currents i_{oA}, i_{oB} and i_{oC}.

3.1 Control of the series transformer currents

As the state-space vector representation is used, from Fig. 2 and Fig. 3, the dynamics of the IMC output currents (i_{oA}, i_{oB}, i_{oC}) are obtained in αβ coordinates ($i_{o\alpha}$, $i_{o\beta}$) (12), and depend on the series

transformer voltages $v_{se\alpha\_IMC}$, $v_{se\beta\_IMC}$ and on the IMC output voltages $v_{o\alpha}$, $v_{o\beta}$. The parasitic resistance of inductance L is represented by r_L.

$$\begin{cases} \dfrac{di_{o\alpha}}{dt} = \dfrac{v_{o\alpha}}{L} - \dfrac{r_L}{L} i_{o\alpha} - \dfrac{v_{se\alpha\_IMC}}{L} \\ \dfrac{di_{o\beta}}{dt} = \dfrac{v_{o\beta}}{L} - \dfrac{r_L}{L} i_{o\beta} - \dfrac{v_{se\beta\_IMC}}{L} \end{cases} \quad (12)$$

The series transformer currents $i_{o\alpha\beta}$ are controlled by a nonlinear approach to ensure that they follow their references $i_{o\alpha\beta ref}$. The control goal is to guarantee: $i_{o\alpha\beta} = i_{o\alpha\beta ref}$. Thus, by analyzing the sign of the current error $e_{i\alpha\beta} = i_{o\alpha\beta ref} - i_{o\alpha\beta}$ and assuming that the error value should be bounded by Δ, the controller command actions are:

- If $e_{i_{\alpha\beta}} > \Delta \Rightarrow i_{o_{\alpha\beta ref}} > i_{o_{\alpha\beta}} \Rightarrow i_{o_{\alpha\beta}} \uparrow$ (must increase)
- If $e_{i_{\alpha\beta}} < -\Delta \Rightarrow i_{o_{\alpha\beta ref}} < i_{o_{\alpha\beta}} \Rightarrow i_{o_{\alpha\beta}} \downarrow$ (must decrease)
- If $-\Delta < e_{i_{\alpha\beta}} < \Delta \Rightarrow i_{o_{\alpha\beta ref}} \approx i_{o_{\alpha\beta}} \Rightarrow i_{o_{\alpha\beta}} \leftrightarrow$ (held constant)

Then the state-space vectors are chosen and the switching gate signals are generated to meet these requirements [12].

3.2 Voltage control at the PCC

The RMS values of the three-phase voltages at the PCC should be bounded by standard EN50160 [1].

The PCC voltages will be controlled using a linear approach and the system equations are obtained in a *dq* reference frame synchronous with the grid voltages, using Park transformation. Then, in the established *dq* reference frame, the grid voltages are [12]:

$$\begin{cases} v_{gd} = \sqrt{3} V \\ v_{gq} = 0 \end{cases} \quad (13)$$

To obtain the necessary parameters to control these voltages it is assumed that the IMC currents are controlled and may be represented as equivalent current sources. A simplified diagram used to design the voltage PI controllers is represented in Fig. 5.

From Fig.5 the block diagram of the voltage controllers is obtained (Fig. 6), where the power electronic converter (IMC) is represented as a first order transfer function [13], and α_v represents the voltage sensor gain.

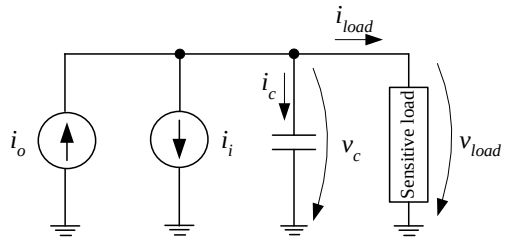

Fig. 5. Simplified scheme of the voltage regulation system.

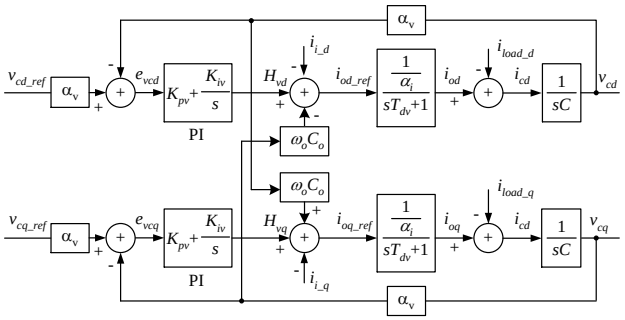

Fig. 6. Block diagram of the PCC voltage controller

From Fig. 6 it is possible to obtain the closed-loop transfer function (14).

$$\frac{v_{c_{dq}}(s)}{v_{c_{dq\_ref}}(s)} = \frac{\dfrac{s K_{pv} + K_{iv}}{T_{dv} C \alpha_i}}{s^3 + \dfrac{1}{T_{dv}} s^2 + \dfrac{K_{pv} \alpha_v}{T_{dv} C \alpha_i} s + \dfrac{K_{iv} \alpha_v}{T_{dv} C \alpha_i}} \quad (14)$$

To determine the Proportional-Integral (PI) gains K_{pv} and K_{iv} (15) the denominator of (14) is compared to the third order ITAE polynomial.

$$\begin{cases} K_{pv} = \dfrac{2.15 C \alpha_i}{\alpha_v T_{dv} (1.75)^2} \\ K_{iv} = \dfrac{C \alpha_i}{\alpha_v T_{dv}^2 (1.75)^3} \end{cases} \quad (15)$$

The values of capacitors C were chosen to be 0.1 mF. Then, assuming the response time of the voltage controller T_{dv}, the values obtained for the PI gains are presented in table IV.

TABLE IV. VOLTAGE CONTROLLER PARAMETERS

Voltage controller parameters		
T_{dv} **[ms]**	K_{iv}	K_{pv}
0.25	2980	2.81

3.3 Power factor control in the IMC

In the chosen *dq* reference frame (13), the grid currents and voltages are in phase when i_{gq}=0. Considering the dynamics of the filter [12], current i_{gq} is controlled by a nonlinear approach to ensure that it follows its reference i_{gqref}. The control goal is to guarantee: i_{gq}=i_{gqref}. Then, analyzing the sign of

the current error $e_{igq} = i_{gqref} - i_{gq}$ and assuming that the error value should be bounded by Δ, the controller command actions are:

- If $e_q < -\Delta \Rightarrow i_{qref} < i_q \Rightarrow i_q \downarrow$ (must decrease)
- If $e_q > \Delta \Rightarrow i_{qref} > i_q \Rightarrow i_q \uparrow$ (must increase)

With this reasoning, it is possible to choose the most adequate vector to apply to the converter, using the approach proposed in [12].

3 Simulation of the Proposed System

The developed system was tested in MATLAB Simulink software for different operating conditions, and supplying a 50kVA three-phase load.

3.1 Grid conditions and load scenarios

The main goal of the UPQC is to guarantee that the load voltage is bounded by the limits defined in standard EN50160, presenting a THD lower than 8%.

In this context, three possible grid operating conditions to assess the capabilities of the UPQC in restoring the voltage to normative values have been tested. For each of these grid operating conditions, two different load scenarios with different percentages of nonlinear loads have been considered:

- Load scenario 1 where 20% of the loads are nonlinear;
- Load scenario 2 where the percentage of non-linear loads has been increased to 40%.

To have a more realistic simulation, it has been assumed that in the connection to the LV grid, the short-circuit power is S_{cc}=75MVA and X/R=0.5. Also it is considered that the grid is not supplying a perfectly sinusoidal waveform: the 5th harmonic contribution is weighted 3% of the fundamental harmonic. As a result, from (2) the THD of the grid voltage at no-load is THD_v=3%.

In the simulations two results will be presented: with and without the UPQC. The aim is to show how the UPQC is able to improve PQ. The main results are presented in tables V, VI and VII. With these results it is possible to see that the UPQC is a valuable contribution to improve the PQ.

3.2 Results obtained under nominal grid operating conditions

According to the standard EN 50160, the rated value of the LV grid phase to neutral voltage is 230V. This voltage is bounded by an upper limit of +10% of this value (253V) and a lower limit of -10% of this value (207V).

In nominal conditions the grid voltage value is bounded by the standard limits. Still, even in this case, the UPQC represents an advantage because, as table V shows, it guarantees lower THD_v in the load, as well as lower THD_i and higher P_F in the grid.

TABLE V. SIMULATION RESULTS WITH AND WITHOUT UPQC IN NOMINAL OPERATING CONDITIONS

Nominal operating conditions					
PQ parameters / Test Scenario	THD_v [%]	THD_i [%]	V_{load} [V]	$Ig_{\_RMS}$ [A]	P_F
UPQC scenario 1	2.17	2.30	228.78	79.61	0.99
Without UPQC scenario 1	3.00	7.08	230.00	79.01	0.98
UPQC scenario 2	2.54	2.23	224.69	79.54	0.99
Without UPQC scenario 2	3.00	10.6	230.00	86.87	0.96

The grid currents are shown in Fig. 7 under nominal grid operating conditions, without UPQC and considering a non-linear load. The waveforms were obtained for scenario 2 which is the most critical, with a higher percentage of nonlinear loads connected to the PCC. In this case without compensation the grid currents are the same as the load currents.

Fig. 8 shows the results obtained in the same conditions but using the UPQC for compensation. The grid currents in Fig. 8a) are nearly sinusoidal and they are in phase with the load voltages, as shown in Fig. 8b).

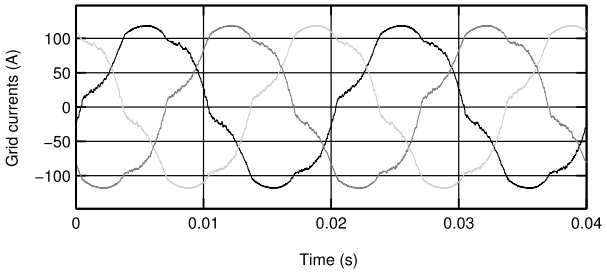

Fig. 7. Grid currents under nominal grid operating conditions, without UPQC and considering a non-linear load of 40 %.

Comparing figures 7 and 8 it can be seen that with the UPQC there is a clear improvement in the grid current waveform, with a visible reduction of THD_i (table V).

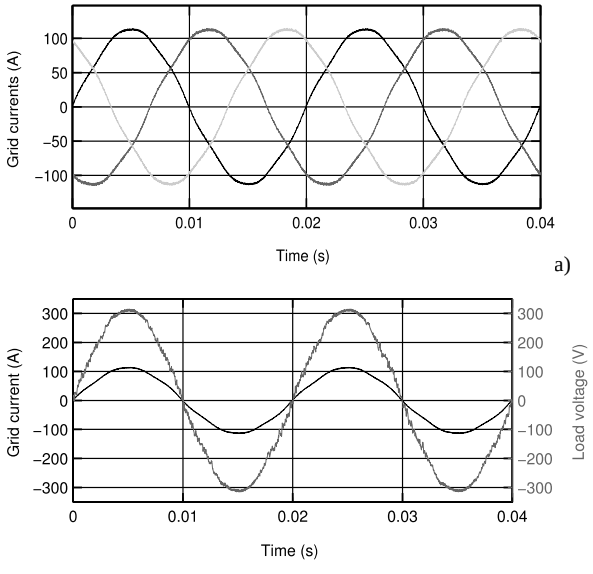

Fig. 8. Nominal grid operating conditions with UPQC and a non-linear load of 40%. a) Grid currents. b) Grid current and load voltage.

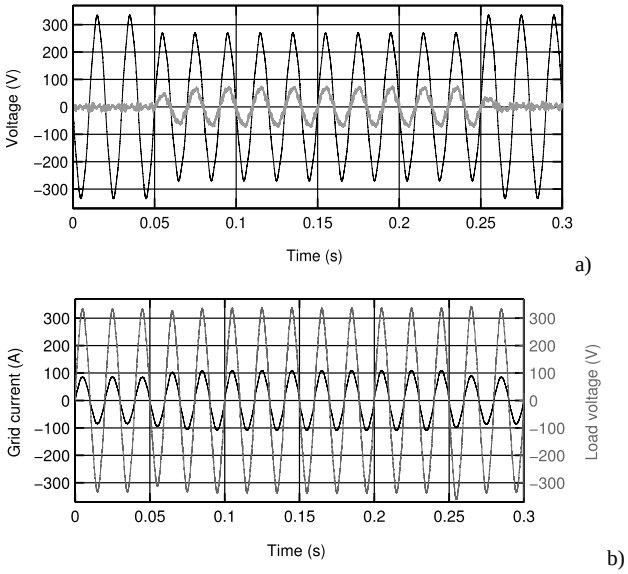

Fig. 9. Waveforms for a 20 % sag with compensation from the UPQC: a) Grid (black) and series transformer (grey) voltages. b) Grid current and load voltage.

3.3 Results obtained for sag operating conditions

The results of table VI have been obtained for a 25% sag depth. From table VI, without the UPQC the voltage applied to the load is equal to the supply voltage. As a result, when there is a sag it will propagate through the grid and will affect the sensitive load.

TABLE VI. SIMULATION RESULTS WITH AND WITHOUT UPQC IN SAG CONDITIONS

Sag conditions					
PQ parameters / Test Scenario	THD_v [%]	THD_i [%]	V_{load} [V]	Ig_{RMS} [A]	P_F
UPQC scenario 1	2.15	2.25	219.58	100.11	0.99
Without UPQC scenario 1	3.00	7.08	172.50	59.33	0.98
UPQC scenario 2	2.21	2.29	210.89	100.12	0.99
Without UPQC scenario 2	3.00	10.59	172.50	65.19	0.96

With the obtained results it can be clearly seen that without the UPQC the voltage is not within the limits defined by standard EN 50160. With the UPQC, the voltage in the load always complies with the required values.

Considering the P_F it is visible that the UPQC guarantees an improvement of this PQ parameter. In all the UPQC operating scenarios it was possible to guarantee a nearly unitary P_F in the connection to the grid.

Fig. 9 presents some of the results obtained for a sag of 20 % depth, starting at t=0.05s. The THD_v of the grid voltages is 3%, and a linear load is considered.

From the obtained results, it can be seen that the load is not affected by the sag, as the series transformer is able to supply the necessary voltage to compensate the sag.

3.4 Results obtained for swell operating conditions

The results of table VII have been obtained for a 25% swell.

TABLE VII. SIMULATION RESULTS WITH AND WITHOUT UPQC IN SWELL CONDITIONS

Swell conditions					
PQ parameters / Test Scenario	THD_v [%]	THD_i [%]	V_{load} [V]	I_{g_RMS} [A]	P_F
UPQC scenario 1	2.21	2.10	233.71	65.25	0.99
Without UPQC scenario 1	3.00	7.07	287.50	98.74	0.98
UPQC scenario 2	2.48	2.19	230.19	65.24	0.99
Without UPQC scenario 2	3.00	10.59	287.50	108.61	0.96

Without UPQC, the voltage applied to the load is equal to the supply voltage. As a result, when there is a swell, it will propagate through the grid and will affect the sensitive load. With the UPQC, the voltage in the load always complies with the required values. Also, the UPQC clearly contributes to improve the P_F.

4 Conclusions

The main aim of this work was to propose a UPQC based on an IMC. The obtained results show that the proposed solution can be used to improve PQ both

in the sensitive load and in the connection to the grid.

With the proposed topology it was possible to restore the voltage applied to the sensitive load to the values bounded by standard EN 50160 while reducing the current harmonic contents, reducing the current THD in the connection to the grid and guaranteeing a nearly unitary P_F.

Acknowledgments

This work was supported by national funds through Fundação para a Ciência e a Tecnologia (FCT) with reference UID/CEC/50021/2013 and the Belgian Fund for training in Research in Industry and in Agriculture (F.R.I.A.).

References:

[1] Standard EN 50160; Voltage characteristics of electricity supplied by public electricity networks, Jul. 2010.

[2] B. Renders, K. Gussemé, W. Ryckaert, K. Stockman, L. Vandevelde, M. Bollen, Distributed generation for mitigating voltage dips in low-voltage distribution grids, *IEEE Trans. Power Del.*, vol. 23, no.3, pp. 1581-1588, Jul. 2008.

[3] P. Gambôa, J. Silva, S. Pinto, and E. Margato, Predictive optimal control for a dynamic voltage restorer with flywheel energy storage, in *Proc. 2009 IEEE 35th Annu. Conf. of Industrial Electronics Society*, pp. 759-764.

[4] V. Khadkikar, Enhancing electric power quality using UPQC: a compreensive overview, *IEEE Trans. Power Electron.*, vol. 27, no. 5, pp. 2284-2297, May 2012.

[5] F. Wang, J. Duarte, and M. Hendrix, Grid-interfacing converter systems with enhanced voltage quality for microgrid application – concept and implementation, *IEEE Trans. Power Electron.*, vol. 26, no. 12, pp. 3501-3513, Dec. 2011.

[6] P. Szczesniak, J. Kaniewski, Power electronics converters without DC storage in the future electrical power network, *Elect. Power Syst. Research*, vol. 129, pp.194-207, Dec. 2005.

[7] C. Garcia, M. Rivera, M. Lopes, J. Rodriguez, R. Pena, P. Wheeler, J. Espinoza, A simple control strategy for a four-leg indirect matrix converter, IEEE Trans. Power Electron., vol. 20, no.4, pp. 2275-2287, Apr. 2015.

[8] J. Silva, V. Pires, S. Pinto, J. Barros, Advanced control methods for power electronics systems, *Mathem. and Comp. in Simul.*, Elsevier, vol. 63, no. 3, pp. 281-295, Nov. 2003.

[9] J. Ferreira and S. Pinto, P-Q decoupled control scheme for unified power flow controllers using sparse matrix converters, *5th Intern. Conf. on the European Electricity Market*, May 2008.

[10] J. Kolar, M. Baumann, F. Schafmeister, H. Ertl, Novel three-Phase AC-DC-AC sparse matrix converter, Proc. IEEE Conf. APEC'2002, vol. 2, pp 777-791, 2002.

[11] A. Sahoo, K. Basu, and N. Mohan, Systematic input filter design of matrix converter by analytical estimation of RMS current ripple, *IEEE Trans. Ind. Electron.*, vol. 62, no. 1, pp. 132-143, Jan. 2015.

[12] S. F. Pinto, and J. F. Silva, Direct control method for matrix converters with input power factor regulation, IEEE 35th Annu. *Power Electron. Specialists Conf.*, PESC 04, vol. 3, pp. 2366-2372, Jun. 2004.

[13] S. Pinto, and J. Silva, Constant frequency sliding mode and PI linear controllers for power rectifiers: a comparison, *IEEE Trans. Ind. Electron.*, vol. 46, no.1, pp. 39-51, Feb. 1999.